Research Article

Molecular Cancer Therapeutics

Effect of the Specific Src Family Kinase Inhibitor Saracatinib on Osteolytic Lesions Using the PC-3 Bone Model

Joy C. Yang[1], Lanfang Bai[1], Stanley Yap[1], Allen C. Gao[1,3], Hsing-Jien Kung[2,3], and Christopher P. Evans[1,3]

Abstract

The hematogenous metastatic spread of prostate cancer is preferentially to bone and can result in significant patient morbidity. Although these metastatic lesions are typically osteoblastic, bone resorption is believed to have a prerequisite role in their development. Src kinase has been identified to contribute to prostate cancer tumor growth and metastasis. In addition, Src is also essential in bone metabolism, especially in bone resorption. We hypothesized that inhibiting Src activity with the specific Src family kinase inhibitor saracatinib (AZD0530) would inhibit tumor cell growth and osteoclast differentiation in the tumor-bone interface, thus providing a new approach for advanced prostate cancer. We found that saracatinib inhibited PC-3 cell growth and invasion in a dose-dependent manner. Phosphorylation of Src, focal adhesion kinase, and P38 kinases was inhibited by saracatinib at the submicromolar range. Saracatinib also inhibited the expression and secretion of invasion-related molecules interlukin-8, urokinase-type plasminogen activator, and matrix metalloprotease-9. Receptor activator of NF-κB ligand (RANKL)–induced osteoclastogenesis and signaling were inhibited by saracatinib in both macrophages and PC-3 cells. In *in vivo* studies, control mice developed more severe osteolytic lesions compared with the treatment group. Immunohistochemical and biochemical assays of bone metabolites confirmed that saracatinib preserved bone architecture in the presence of prostate cancer tumor cells. In summary, we have shown the inhibition of PC3 cell growth and invasion by saracatinib. Src inhibition also blocked the RANKL stimulatory pathway in osteoclasts and PC3 cells. The inhibition of Src thus targets multiple sites involved in prostate cancer bone metastasis, which may offer a therapeutic advantage in treating advanced prostate cancer. *Mol Cancer Ther; 9(6); 1629–37. ©2010 AACR.*

Introduction

Prostate cancer skeletal involvement is the most common metastatic site in advanced-stage disease, observed in up to 80% of patients (1). Unlike other solid tumor metastases that cause bone loss, prostate cancer bone metastases result in an overall increase in bone mass or osteoblastogenesis. It is not entirely clear why prostate tumor cells localize to the bone environment. The enriched blood source and complex growth factors in the bone marrow provide a good soil for circulating prostate tumor cells to seed and multiply. Growth factors released from tumor cells support increase of both bone resorption and formation (2). Increased osteoclastogenesis has been detected in prostate cancer bone metastases (3). The initial osteoclast-mediated osteolytic process is critical to the subsequent osteoblastic lesions, and a metastatic phenotype consists of a combination of both bone resorption and formation (4–6). A vicious cycle in the tumor cell–bone interface drives the metastasis, whereby growth factors secreted by tumor cells stimulate osteoclast formation and matrix turnover. This osteoclastic resorption causes the local release of more growth factors that in turn activate tumor growth. Src, a non–receptor tyrosine kinase, is implicated in the cross-talk in this tumor-bone interface through its central role in bone metastasis and tumor progression.

The importance of Src kinase in osteoclasts was first discovered in Src knockout mice in which defective osteoclastic resorption gave rise to the phenotype of osteopetrosis and toothlessness (7, 8). In bone formation and remodeling, Src is activated in osteoclasts upon attachment of cells to bone matrix through integrin receptors, and activated Src recruits several signaling proteins for motility and cytoskeletal rearrangement (9, 10). Src is also important in the receptor activator of NF-κB ligand (RANKL)/RANK/osteoprotegerin signaling pathway, which contributes to osteoclast differentiation. Membrane-bound or soluble RANKL binds to its receptor RANK to initiate the signaling cascade leading to osteoclast activation. Upon ligand binding, RANK recruits the tumor necrosis factor receptor–associated factors to its

Authors' Affiliations: Departments of [1]Urology and [2]Biochemistry and Molecular Medicine and [3]Cancer Center, University of California at Davis, Sacramento, California

Corresponding Author: Christopher Evans, Department of Urology, University of California Davis School of Medicine, Suite 3500, 4860 Y Street, Sacramento, CA 95817. Phone: 916-734-7520; Fax: 916-734-8904. E-mail: cpevans@ucdavis.edu

doi: 10.1158/1535-7163.MCT-09-1058

cytoplasmic domain (11–13). This crucial step leads to activation of NF-κB (14), mitogen-activated protein kinase (MAPK; refs. 15–17), and Src (10, 18–20) signaling pathways in osteoclasts. In addition to osteoclast activation, Src recruits phosphatidylinositol-3 kinase and activates the Akt/mammalian target of rapamycin pathway to promote osteoclast survival (21, 22).

Our previous studies showed that Src kinase plays an important role in promoting androgen-independent prostate tumor growth (23–26). Upregulation of Src family kinase (SFK) activities has been reported in 28% of androgen-independent prostate cancer patients (27). Moreover, this enhanced SFK activity correlated with prostate cancer bone metastasis and a significant decrease in survival. The specific SFK inhibitor saracatinib (AZD0530) inhibited the activities of Src and focal adhesion kinase (FAK) kinases and their downstream substrates. Phosphorylation of Src and FAK was inhibited by saracatinib in the nanomolar range. As a result, tumor metastasis was profoundly inhibited in an animal study using castration-resistant LNCaP expressing neuropeptide gastrin-releasing peptide (LNCaP-GRP cells; ref. 26).

We proposed to use saracatinib not only as an adjunct to hormone ablation therapy and to target patients with upregulation in SFK activity but also for patients with bone metastasis. In this study, we use PC-3 cells for their ability to steadily induce osteolysis when implanted in the mouse tibia. In addition to downregulation of cell proliferation and migration as reported before, saracatinib inhibited the expression of interleukin-8 (IL-8), urokinase plasminogen activator (uPA), and matrix metalloprotease-9 (MMP-9), and PC-3 invasion, which altogether suggests that saracatinib may inhibit prostate tumor cell invasion into the bone matrix. Induced differentiation of macrophage cells into osteoclasts by RANKL was inhibited by saracatinib, as was the activation of Src, P38, and IκB-α in PC-3 cells—events generally mediated through RANKL stimulation. Our animal study further shows the ability of saracatinib to retard osteolytic lesions, a potential therapeutic advantage in treating patients with prostate cancer.

Materials and Methods

Cell lines

The PC-3 prostate cancer cell line was obtained from the American Type Culture Collection and cultured in RPMI 1640 supplemented with 5% fetal bovine serum (FBS). RAW264.7 cells, a murine osteoclast precursor, was from the American Type Culture Collection and kept in DMEM with 10% FBS.

Proliferation assay

PC-3 cells were seeded (2,000 per well) in triplicates in 96-well plates. Varied concentrations of saracatinib (0–5 μmol/L, AstraZeneca) were added, and cell growth was monitored by 3-(4,5-dimethylthiazol-2-yl)-2,5-diphenyl tetrazolium bromide (MTT, Sigma) assay at 1, 3, and 5 days posttreatment.

Invasion assay

Invasion assays were done according to procedures described by Lochter and colleagues (28) and modified as follows. PC-3 cells (1×10^5) were suspended in growth medium containing dimethyl sulfoxide or various concentrations of saracatinib (8 nmol/L to 5 μmol/L in 5-fold increments) into the cell culture inserts containing 8 μmol/L pores for 24-well plates. The inserts were coated with Matrigel (2–3 mg/mL protein) and allowed to solidify before cell plating. The lower chambers were filled with 300 μL of growth medium containing control or drugs of corresponding concentrations. After 72 hours in culture, cells were fixed with 5% glutaraldehyde in PBS and stained with 0.5% toluidine blue in 2% Na_2CO_3. Only cells that penetrated the membrane were counted in five microscopic fields per filter.

Osteoclast differentiation from RAW264.7 cells

Osteoclast formation assay was done by plating 5×10^4 RAW264.7 cells per well in 24-well plates in DMEM with 10% FBS for 4 days. Soluble RANKL (100 ng/mL, Santa Cruz Biotechnology) was added to stimulate osteoclast differentiation, and saracatinib (1 μmol/L) was added for inhibition. At the end of incubation, the cells were fixed and stained with a tartrate-resistant acid phosphatase (TRAP) staining kit (Acid Phosphatase Kit 387-A, Sigma), and TRAP-positive staining osteoclasts (multinuclear cells with > 3 nuclei) were counted in five different microscopic fields.

Reverse transcriptase-PCR and quantitative reverse transcriptase-PCR

Total RNA was isolated from PC-3 cells treated with or without 1 μmol/L of saracatinib at different time points (0, 6, and 24 hours). Two micrograms of RNA were reverse transcribed into cDNA followed by PCR using specific primers. Quantitative PCR was done in iCycler with SYBR Greener QPCR iCYLer (Invitrogen), and the output was normalized against the controlled amplification products with glyceraldehyde-3-phosphate dehydrogenase.

Gel zymography

MMP-9 activity was analyzed with gelatin zymography as described below. Conditioned media harvested from PC-3 treated with or without various concentrations of saracatinib for 48 hours were concentrated through centrifugation using Microcon concentrators (Amicon). Concentrated conditioned medium was normalized to total cellular protein (equivalent to 100 μg per loading), then subjected to electrophoresis in gels containing 0.2% gelatin without denaturing. After electrophoresis, the gels were washed in 2% Triton X-100 for 30 minutes and incubated in 50 mmol/L Tris-HCl (pH 7.4), 200 mmol/L NaCl, and 10 mmol/L $CaCl_2$ at 37°C

overnight. Gels were then stained with Coomassie brilliant blue R-250 and destained with methanol/HOAc/H_2O (4:1:5) until clear bands appeared.

Western blot analyses

PC-3 cells were cultured to 70% confluency and treated with various concentrations of saracatinib for 1 hour. Cells were then lysed in ice-cold buffer (Tris 25 mmol/L, $MgCl_2$ 10 mmol/L, β-glycerolphosphate 25 mmol/L, Na_3VO_4 5 mmol/L, and protease inhibitor cocktail) and ruptured through three freeze-thaw cycles. Cell lysates were separated from debris by centrifugation, and protein concentrations were determined by the bicinchoninic acid assay (Pierce). Thirty micrograms of protein were separated on SDS-PAGE and electrotransferred onto polyvinylidene difluoride membrane. Immunoblotting was done by incubating membranes with the primary antibodies overnight, followed by 1 hour of secondary antibody incubation. Signals were detected by SuperSignal West Pico CL (Pierce) coupled with X-ray film exposure. For inhibition of the RANKL/RANK pathway, PC-3 cells were serum-starved for 48 hours before stimulation by RANKL (100 ng/mL) in 2% FBS medium for 0, 2, 5, 15, 30, and 60 minutes. SFK inhibitor saracatinib (1 μmol/L) was added to the last three time points together with RANKL. At the end of treatments, cells were collected as described, and lysates were subjected to gel electrophoresis. Antibodies against p-Src (Tyr416), total Src (36D10), Akt, p-Akt (Ser473), P38, p-P38 (Thr180/Tyr182, 28B10), extracellular signal-regulated kinase 1/2 (Erk1/2; p44/42MAPK), IκBα (44D4), and p-IκBα (Ser32, 14D4) were purchased from Cell Signaling; anti–p-FAK (Y397) was from BD Biosciences; and anti–p-FAK (Y861) was from Affinity BioReagents.

In vivo inhibition study

PC-3 cells (2×10^5) mixed with equal amounts of Matrigel in a final volume of 10 μL were injected into 24 male severe combined immunodeficient (SCID) mice tibia. Intratibial injections were done using a 29-gauge, 1/2-inch needle inserted through the tibial plateau of the flexed knee. After animals recuperated from the surgery (7 days later), they were randomly divided into two groups and given oral saracatinib (25 mg/kg) or buffer (0.5% hydroxypropyl methylcellulose and 0.1% Tween 80) daily for 8 weeks from implantation. Anesthetized mice had bone lesions monitored weekly

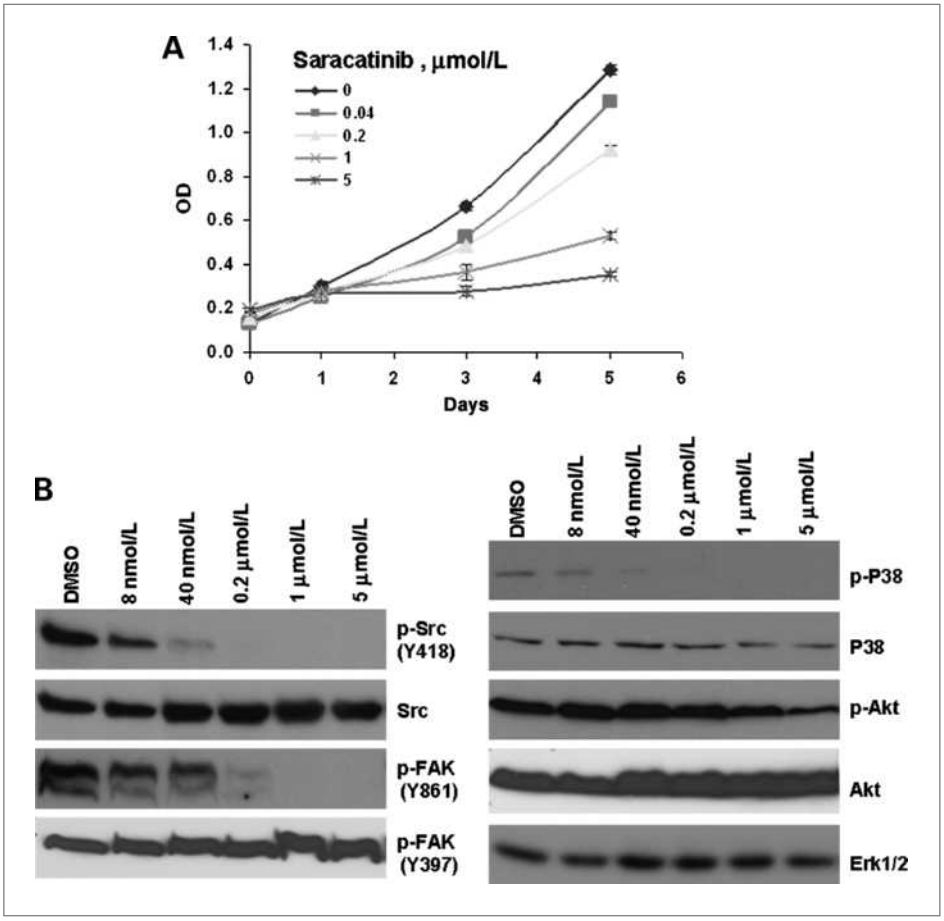

Figure 1. Inhibition of PC-3 cell proliferation and downstream signaling by saracatinib. A, PC-3 cells were seeded in 96-well microtiter plates. After day 0 readings, cells were treated with various amounts of saracatinib or dimethyl sulfoxide (DMSO) only. Cell viability was measured by the MTT assay to produce the dose-response growth inhibition curve. Means of triplicate experiments were plotted; bars, SEM. B, the SFK inhibitor saracatinib inhibited Src and FAK activation and downstream signaling. A saracatinib concentration of 8 nmol/L was sufficient to inhibit the activation of Src, FAK, and P38 to different degrees. Akt phosphorylation only started to show reduction with 1 μmol/L or more of saracatinib. The phosphorylation of Erk1/2 was below detection; however, the levels of total Erk1/2 in each sample confirmed equal loading and unchanged expression of the kinase.

using Faxitron (Faxitron X-ray Corp.). At the end of 8 weeks, animals were sacrificed with collection of urine, sera, and tibias for biochemical and pathologic analyses. The tibias were fixed in 10% buffered formalin for 2 days, followed by decalcification in 10% EDTA solution for 2 weeks at room temperature with occasional stirring and solution changes. Specimens were paraffin embedded, sectioned, and stained with H&E and TRAP. Histomorphometric analysis was done on an Olympus system. The number of large active osteoclasts (TRAP-positive osteoclasts with three or more nuclei) per millimeter of tumor-bone interface was measured from 4-week control and treatment bone sections in five different fields at 200× magnification. Total tumor percentage in the medullary cavity of each bone from 8-week controls and treatment samples was measured at 40× magnification.

Serum pyridinoline and urine helical peptide assays

The pyridinoline cross-links and helical peptides representing the degree of bone resorption were measured by EIA assays (Metra Serum pyridinoline assay and Metra Helical Peptide EIA Kit, Quidel).

Statistics

Statistical analyses were done using unpaired Student's *t* tests (StatView, SAS Institute). Significant results were determined as $P \leq 0.05$.

Results

SFK inhibitor saracatinib inhibits PC-3 growth

We have reported that SFK inhibitor saracatinib efficiently inhibits the growth of most prostate cancer cells, LNCaP, PC-3, DU-145, and CWR22Rv1, with IC_{50} values in the low micromolar range (29). PC-3 cells are especially sensitive to saracatinib with an IC_{50} of 0.7 μmol/L (Fig. 1A). Inhibition of phosphorylation of Src kinase and its immediate substrate FAK was achievable with submicromolar levels of saracatinib, as was the case for MAPK-P38. Inhibition of Akt required higher doses of saracatinib, implying an indirect relationship of Src and Akt (Fig. 1B).

SFK inhibitor saracatinib inhibits PC-3 invasion

Saracatinib is very potent in inhibiting PC-3 cell migration with an IC_{50} value of ~50 nmol/L. This

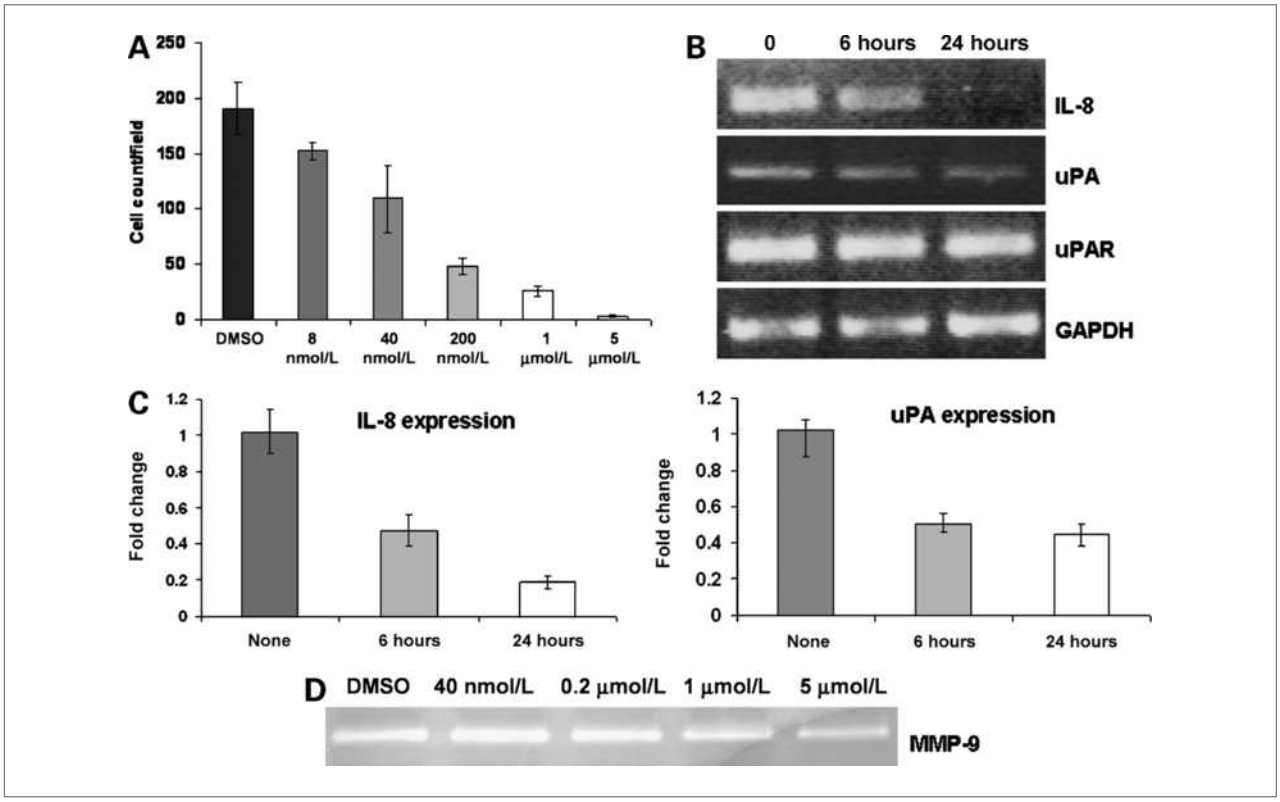

Figure 2. The effect of saracatinib on invasion and invasion-related molecules, IL-8, uPA, and MMP-9. A, invasion assay was set as described in Materials and Methods. Saracatinib inhibited PC-3 invasion through Matrigel in a dose-dependent manner. B, expression of IL-8 and uPA in saracatinib (1 μmol/L)–treated PC-3 cells was determined by reverse transcriptase-PCR. Inhibition of Src kinase resulted in reduction of IL-8 and uPA expression, but not uPA receptor (uPAR). These inhibitions were further quantitated by quantitative PCR (C) for IL-8 and uPA. D, inhibition of MMP-9 secretion by saracatinib was assayed by gelatin zymography. In-gel digestion of gelatin decreased as the doses of saracatinib increased, indicating reduction of MMP-9 secretion. Loading of concentrated conditioned medium was normalized by the amounts of total protein from each sample point.

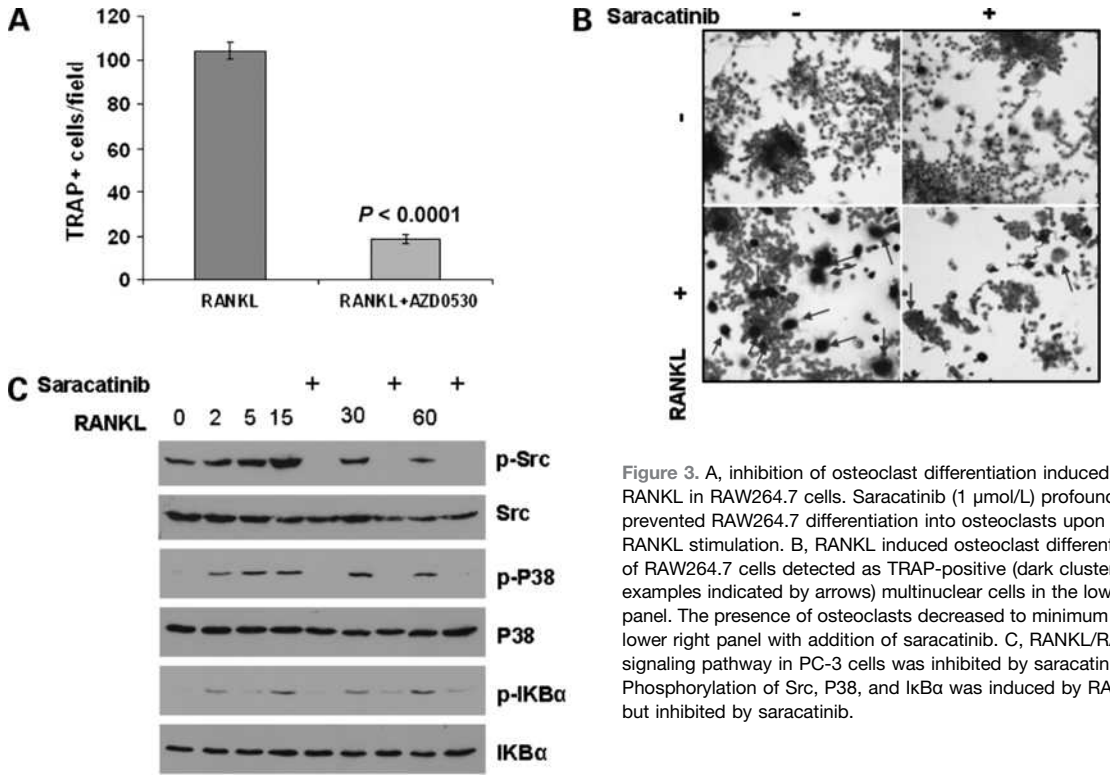

Figure 3. A, inhibition of osteoclast differentiation induced by RANKL in RAW264.7 cells. Saracatinib (1 μmol/L) profoundly prevented RAW264.7 differentiation into osteoclasts upon RANKL stimulation. B, RANKL induced osteoclast differentiation of RAW264.7 cells detected as TRAP-positive (dark clusters, examples indicated by arrows) multinuclear cells in the lower left panel. The presence of osteoclasts decreased to minimum in the lower right panel with addition of saracatinib. C, RANKL/RANK signaling pathway in PC-3 cells was inhibited by saracatinib. Phosphorylation of Src, P38, and IκBα was induced by RANKL but inhibited by saracatinib.

SFK inhibitor also blocks PC-3 penetration through Matrigel in invasion assay (Fig. 2A). After 3 days, cell invasion was reduced to 57% and 25% of control in the presence of 40 and 200 nmol/L of saracatinib, respectively. PC-3 cells remained 78% and 73% viable using the same concentrations of inhibitor over the same period of time; thus, the reduction was indeed the effect of saracatinib on cell invasion. The expression of invasion-related molecules IL-8 and uPA was inhibited by saracatinib in a timely manner (Fig. 2B). Treatment of PC-3 cells with 1 μmol/L of saracatinib reduced IL-8 transcripts to 30% in 6 hours and to 18% in 24 hours (Fig. 2C). The same treatment halved uPA expression in 6 hours and further decreased to 44% after 24 hours. The level of uPA receptor was only slightly reduced (to around 85%) after 24 hours of treatment. MMP-9 activity in PC-3 cultured medium was inhibited by saracatinib in a dose-responsive manner (Fig. 2D).

Saracatinib inhibits RANKL-induced osteoclastogenesis and signaling

Murine macrophage RAW264.7 precursors for osteoclasts may be stimulated by RANKL (100 ng/mL) to undergo osteoclast differentiation. Addition of 1 μmol/L saracatinib drastically inhibited osteoclast differentiation by limiting the number of TRAP-stained multinuclear osteoclasts to less than 18% of control (Fig. 3A). Treating RAW264.7 cells with this concentration of saracatinib alone did not cause massive cell death as shown in the staining (Fig. 3B); hence, the reduction in TRAP staining is likely due to inhibition of osteoclast differentiation. It has been reported that functional RANK is expressed in prostate cancer cell lines such as PC-3 and DU-145 (30). The receptors render these prostate cancer cells under the control of bound or soluble RANKL from osteoblasts or stroma to enhance tumor growth in the bone environment. We therefore tested if saracatinib would block the RANKL/RANK pathway in PC-3 cells. Activation of Src, P38, and IκBα (a few representatives from the RANKL/RANK pathway) was detectable at 2 minutes from RANKL addition and peaked within 15 minutes (Fig. 3C). Saracatinib completely blocked phosphorylation of these kinases at 15, 30, and 60 minutes.

In vivo inhibition with a PC-3 tibial model

Based on our *in vitro* observations, we then implanted PC-3 cells into the tibia of SCID mice to study the effect of the Src inhibitor *in vivo*. PC-3 cells cause osteolysis when injected directly into mouse bones (31–33). In our study, osteolysis started to appear in the control group 3 weeks after injection. Radiographs

taken at 4 and 8 weeks (end points) showed that saracatinib significantly inhibited the osteolytic lesion in the treatment group compared with controls (Fig. 4A). At 5 weeks from surgery, 9 of 12 control mice showed osteolytic lesions compared with only 4 in the treatment group. TRAP staining of the tibial samples taken at 4 weeks showed growth of tumor cells leading to loss of bone architecture in the control tibias with characteristic TRAP staining signifying the presence of osteoclasts (Fig. 4B). Most of the tibias from the treatment animals retained bone integrity, bearing no signs of tumor cells or osteoclasts. The osteoclast perimeters from the 4-week bone samples were counted. Saracatinib decreased TRAP-positive osteoclasts in tibias of tumor-bearing mice by >10 fold when compared with controls. At the end of 8 weeks, all but one mouse in the control group developed severe lesions, but only half of the treatment animals had milder lesions. The areas of tumor versus bone were measured from histologic staining and plotted to show that saracatinib reduced this ratio in the treatment group to less than half of controls (Fig. 4C). In addition to bone histomorphometric measurements, the effect of saracatinib on released mouse bone metabolites, such as pyridinoline cross-links in serum and α-helical peptides in urine, were measured. Compared with the control group, treated mice had a 46% reduction in pyridinoline ($P = 0.07$, not statistically significant) and 60% reduction in α-helical peptide ($P < 0.01$; Fig. 4D).

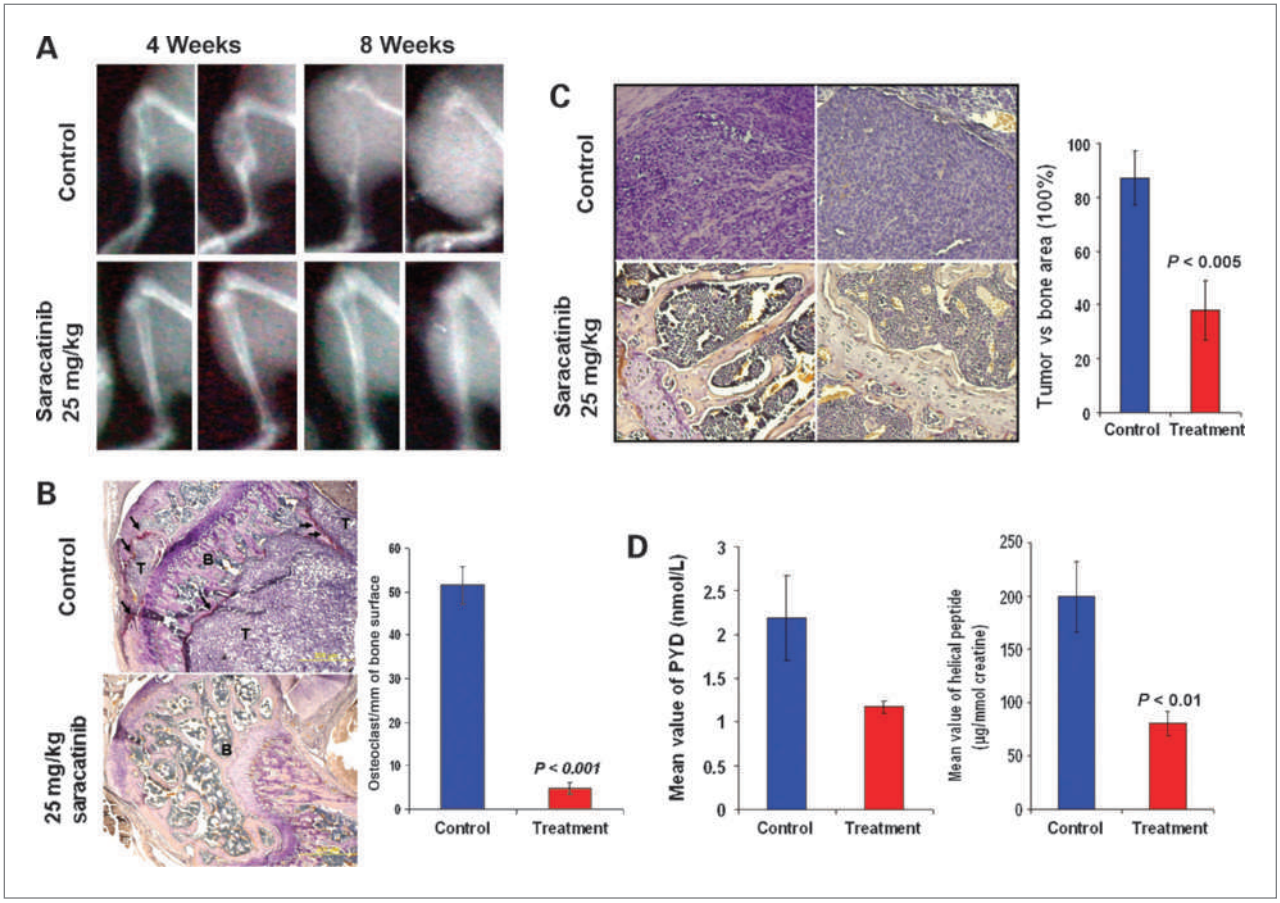

Figure 4. A, radiography of SCID mice tibias implanted with PC-3 cells. Osteolysis was apparent in the tibia from the control group at 4 weeks, whereas the treatment group showed no evidence of osteolysis. At the end of 8 weeks, tibias in all mice but one in the control group showed total destruction. Most of the tibias in the treatment group remained intact. B, sections of tibias from both groups at 4 weeks were stained with TRAP and counterstained with hematoxylin for detecting PC-3 tumor cells in bone and TRAP for osteoclasts. Prostate tumor cells (T) and osteoclasts (arrows) were visibly detected in the control but not in the saracatinib-treated samples. Osteoclast numbers per millimeter bone surface were counted from the 4-week specimens from both control and treatment groups and graphed. C, sections of tibias from the 8-week time point were stained, and the areas of tumor and bone were measured and compared. Stainings of two representatives from each group showed that most tibias from the control group were taken over by tumor, whereas the treatment group still retained the architecture of normal bone. D, biochemical analyses of osteolytic lesions. Detection of serum pyridinoline (PYD) cross-links and urine α-helical peptides in the control and saracatinib-treated animals. The pyridinoline cross-links and helical peptides representing the degree of bone resorption were measured by enzyme immunoassays. Both pyridinoline and helical peptide values in the control were higher than those in the saracatinib-treated groups. The difference in urine helical peptide levels was statistically significant ($P < 0.01$).

Discussion

When standard therapy for advanced prostate cancer using androgen ablation fails, there are limited treatment options for patients with prostate cancer metastatic to bone. At present, bone health is fostered by use of calcium, vitamin D, and zolendronic acid. Unbalanced bone remodeling mediated by prostate tumor cells replaces normal bone tissue with highly disorganized osteoblasts. This leads to predominantly osteoblastic lesions causing significant pain in patients with advanced prostate cancer (34). New therapeutic strategies such as small-molecule inhibitors of signaling pathways responsible for cancer progression are desirable. Src kinase has been implicated in prostate tumor proliferation, migration, survival (23, 35, 36), and progression to castration resistance (26). Many recently developed small-molecule SFK inhibitors, including bosutinib (SKI-606; ref. 37), dasatinib (BMS-354825; refs. 38, 39), and saracatinib are able to reduce the proliferation, migration, and invasion of prostate cancer cell lines *in vitro* and are currently in clinical trials. These inhibitors also decrease prostate cancer growth and metastasis in mouse xenograft studies (26, 29, 39). Recent studies using saracatinib showed that Src has a pivotal role in the formation and activation of human osteoclasts (40) and is involved in breast cancer bone metastasis regardless of the estrogen receptor status (41). A phase I study showed a dose-dependent decrease in bone resorption markers in men receiving saracatinib daily for 2 weeks (42). There were no significant adverse effects. Dasatinib alone and in combination therapy with docetaxel improved bone mineral density in the LNCaP C4-2B tumor–implanted tibias (43).

Using saracatinib, we were able to show a dose-dependent inhibition of proliferation and migration in PC-3 and DU-145 cells (29). Western blot analysis showed that Src phosphorylation in saracatinib-treated cells was reduced in a dose- and time-dependent manner. Intracellular Src-activating proteins, including FAK, P130Cas, and paxillin, were also inhibited, supporting the efficacy of saracatinib in preventing prostate cancer progression. In addition to the previous prostate cancer lines that lack androgen receptor, LNCaP-GRP cells that contain androgen receptor but grow independent of androgen were also sensitive to saracatinib. With the importance of Src in both bone remodeling and prostate cancer tumor progression, the use of Src inhibitors has been proposed in the treatment of prostate cancer bone metastasis (44, 45). In our study, saracatinib has shown specific inhibition of FAK and P38 kinase activation downstream of Src in PC-3 cells. This block in signaling may prevent cytoskeletal rearrangement and migration through FAK (29). We again observed the discrepancy between the doses of saracatinib required for inhibiting Src phosphorylation and cell/tumor growth as discussed in our previous article (29). In addition to speculation of partial inhibition of Src kinase on growth and its downstream signaling, we recently reported that saracatinib induced macroautophagy in cells to spare them from apoptosis by inhibiting the phosphoinositide 3-kinase/Akt/mammalian target of rapamycin pathway (46). Blocking autophagy with drugs such as chloroquine significantly improved the efficacy of saracatinib in treating PC-3 subcutaneous tumors, which may also be applicable to bone treatment. Saracatinib reduced the synthesis of IL-8, uPA, and MMP-9, molecules involved in angiogenesis and basement membrane degradation (47), in PC-3 cells, which is consistent with cell invasion inhibition. RANKL secreted from tumor and stroma cells is responsible for osteoclast differentiation in the tumor-bone interface. Using RAW264.7 cells as a model for osteoclast differentiation induced by RANKL, saracatinib significantly inhibited the formation of osteoclasts. Furthermore, the RANKL-induced RANK/RANKL pathway in PC-3 cells was also inhibited by saracatinib along with P38 and IκBα. Finally, *in vivo* experiments showed that progression of PC-3 implants in the metastatic tibial site was inhibited by saracatinib. The inhibition not only prevented proliferation of PC-3 cells but also hindered multiplication of osteoclasts in the bone environment. Osteoclast perimeter counts were significantly lower at the 4-week time point, and the tumor/bone ratio was halved at the end of the *in vivo* study in the inhibitor-treated specimens. Reduction in secretion of bone turnover markers pyridinoline and helical peptides in mice receiving saracatinib was consistent with fewer osteolytic lesions and decreased osteoclast proliferation. Although the majority of advanced prostate cancer patients develop osteoblastic lesions, bone resorption occurs before new bone formation. Our report on the efficacy of saracatinib on inhibiting PC-3 osteolytic bone lesions is applicable to patients with prostate cancer metastatic to bone.

Results presented herein show the utility of saracatinib in advanced prostate cancer with mechanistic and *in vivo* animal studies supporting clinical trials using saracatinib as a treatment for prostate cancer patients with bone metastasis.

Disclosure of Potential Conflicts of Interest

C.P. Evans is a consultant for AstraZeneca. No other potential conflicts of interest were disclosed.

Acknowledgments

We thank Maggie Chiu of Pathology for making sections and staining the animal study samples.

Grant Support

Department of Defense PC10520 and Prostate Cancer Foundation Competitive Award (C.P. Evans).

The costs of publication of this article were defrayed in part by the payment of page charges. This article must therefore be hereby marked *advertisement* in accordance with 18 U.S.C. Section 1734 solely to indicate this fact.

Received 11/23/2009; revised 03/01/2010; accepted 03/25/2010; published OnlineFirst 05/18/2010.

References

1. Bubendorf L, Schopfer A, Wagner U, et al. Metastatic patterns of prostate cancer: an autopsy study of 1,589 patients. Human Pathol 2000;31:578–83.
2. Keller ET, Zhang J, Cooper CR, et al. Prostate carcinoma skeletal metastases: cross-talk between tumor and bone. Cancer Metastasis Rev 2001;20:333–49.
3. Roato I, D'Amelio P, Gorassini E, et al. Osteoclasts are active in bone forming metastases of prostate cancer patients. PLoS ONE 2008;3: e3627.
4. Inoue H, Nishimura K, Oka D, et al. Prostate cancer mediates osteoclastogenesis through two different pathways. Cancer Lett 2005;223: 121–8.
5. Whang PG, Schwarz EM, Gamradt SC, Dougall WC, Lieberman JR. The effects of RANK blockade and osteoclast depletion in a model of pure osteoblastic prostate cancer metastasis in bone. J Orthop Res 2005;23:1475–83.
6. Zhang J, Dai J, Yao Z, Lu Y, Dougall W, Keller ET. Soluble receptor activator of nuclear factor κB Fc diminishes prostate cancer progression in bone. Cancer Res 2003;63:7883–90.
7. Boyce BF, Yoneda T, Lowe C, Soriano P, Mundy GR. Requirement of pp60c-src expression for osteoclasts to form ruffled borders and resorb bone in mice. J Clin Invest 1992;90:1622–7.
8. Soriano P, Montgomery C, Geske R, Bradley A. Targeted disruption of the c-src proto-oncogene leads to osteopetrosis in mice. Cell 1991;64:693–702.
9. Insogna KL, Sahni M, Grey AB, et al. Colony-stimulating factor-1 induces cytoskeletal reorganization and c-src-dependent tyrosine phosphorylation of selected cellular proteins in rodent osteoclasts. J Clin Invest 1997;100:2476–85.
10. Miyazaki T, Sanjay A, Neff L, Tanaka S, Horne WC, Baron R. Src kinase activity is essential for osteoclast function. J Biol Chem 2004; 279:17660–6.
11. Darnay BG, Haridas V, Ni J, Moore PA, Aggarwal BB. Characterization of the intracellular domain of receptor activator of NF-κB (RANK). Interaction with tumor necrosis factor receptor-associated factors and activation of NF-κb and c-Jun N-terminal kinase. J Biol Chem 1998;273:20551–5.
12. Galibert L, Tometsko ME, Anderson DM, Cosman D, Dougall WC. The involvement of multiple tumor necrosis factor receptor (TNFR)-associated factors in the signaling mechanisms of receptor activator of NF-κB, a member of the TNFR superfamily. J Biol Chem 1998;273: 34120–7.
13. Hsu H, Lacey DL, Dunstan CR, et al. Tumor necrosis factor receptor family member RANK mediates osteoclast differentiation and activation induced by osteoprotegerin ligand. Proc Natl Acad Sci U S A 1999;96:3540–5.
14. Iotsova V, Caamano J, Loy J, Yang Y, Lewin A, Bravo R. Osteopetrosis in mice lacking NF-κB1 and NF-κB2. Nat Med 1997;3: 1285–9.
15. David JP, Sabapathy K, Hoffmann O, Idarraga MH, Wagner EF. JNK1 modulates osteoclastogenesis through both c-Jun phosphorylation-dependent and -independent mechanisms. J Cell Sci 2002;115: 4317–25.
16. Matsumoto M, Sudo T, Saito T, Osada H, Tsujimoto M. Involvement of p38 mitogen-activated protein kinase signaling pathway in osteoclastogenesis mediated by receptor activator of NF-κB ligand (RANKL). J Biol Chem 2000;275:31155–61.
17. Wagner EF. Functions of AP1 (Fos/Jun) in bone development. Ann Rheum Dis 2002;61 Suppl 2:ii40–2.
18. Koga S, Yogo K, Yoshikawa K, et al. Physical and functional association of c-Src and adhesion and degranulation promoting adaptor protein (ADAP) in osteoclastogenesis *in vitro*. J Biol Chem 2005;280: 31564–71.
19. Wong BR, Rho J, Arron J, et al. TRANCE is a novel ligand of the tumor necrosis factor receptor family that activates c-Jun N-terminal kinase in T cells. J Biol Chem 1997;272:25190–4.
20. Xing L, Venegas AM, Chen A, et al. Genetic evidence for a role for Src family kinases in TNF family receptor signaling and cell survival. Genes Dev 2001;15:241–53.
21. Glantschnig H, Fisher JE, Wesolowski G, Rodan GA, Reszka AA. M-CSF, TNFα and RANK ligand promote osteoclast survival by signaling through mTOR/S6 kinase. Cell Death Differ 2003;10: 1165–77.
22. Sugatani T, Hruska KA. Akt1/Akt2 and mammalian target of rapamycin/Bim play critical roles in osteoclast differentiation and survival, respectively, whereas Akt is dispensable for cell survival in isolated osteoclast precursors. J Biol Chem 2005;280: 3583–9.
23. Chang YM, Kung HJ, Evans CP. Nonreceptor tyrosine kinases in prostate cancer. Neoplasia (New York, NY) 2007;9:90–100.
24. Guo Z, Dai B, Jiang T, et al. Regulation of androgen receptor activity by tyrosine phosphorylation. Cancer Cell 2006;10:309–19.
25. Lee LF, Guan J, Qiu Y, Kung HJ. Neuropeptide-induced androgen independence in prostate cancer cells: roles of nonreceptor tyrosine kinases Etk/Bmx, Src, and focal adhesion kinase. Mol Cell Biol 2001; 21:8385–97.
26. Yang JC, Ok JH, Busby JE, Borowsky AD, Kung HJ, Evans CP. Aberrant activation of androgen receptor in a new neuropeptide-autocrine model of androgen-insensitive prostate cancer. Cancer Res 2009;69:151–60.
27. Tatarov O, Mitchell TJ, Seywright M, Leung HY, Brunton VG, Edwards J. SRC family kinase activity is up-regulated in hormone-refractory prostate cancer. Clin Cancer Res 2009;15: 3540–9.
28. Lochter A, Srebrow A, Sympson CJ, Terracio N, Werb Z, Bissell MJ. Misregulation of stromelysin-1 expression in mouse mammary tumor cells accompanies acquisition of stromelysin-1-dependent invasive properties. J Biol Chem 1997;272:5007–15.
29. Chang YM, Bai L, Liu S, Yang JC, Kung HJ, Evans CP. Src family kinase oncogenic potential and pathways in prostate cancer as revealed by AZD0530. Oncogene 2008;27:6365–75.
30. Mori K, Le Goff B, Charrier C, Battaglia S, Heymann D, Redini F. DU145 human prostate cancer cells express functional receptor activator of NFκB: new insights in the prostate cancer bone metastasis process. Bone 2007;40:981–90.
31. Kim SJ, Uehara H, Karashima T, Shepherd DL, Killion JJ, Fidler IJ. Blockade of epidermal growth factor receptor signaling in tumor cells and tumor-associated endothelial cells for therapy of androgen-independent human prostate cancer growing in the bone of nude mice. Clin Cancer Res 2003;9:1200–10.
32. Lee YP, Schwarz EM, Davies M, et al. Use of zoledronate to treat osteoblastic versus osteolytic lesions in a severe-combined-immunodeficient mouse model. Cancer Res 2002;62: 5564–70.
33. Miwa S, Mizokami A, Keller ET, Taichman R, Zhang J, Namiki M. The bisphosphonate YM529 inhibits osteolytic and osteoblastic changes and CXCR-4-induced invasion in prostate cancer. Cancer Res 2005; 65:8818–25.
34. Chirgwin JM, Mohammad KS, Guise TA. Tumor-bone cellular interactions in skeletal metastases. J Musculoskelet Neuronal Interact 2004;4:308–18.
35. Kopetz S, Shah AN, Gallick GE. Src continues aging: current and future clinical directions. Clin Cancer Res 2007;13:7232–6.
36. Saad F. Src as a therapeutic target in men with prostate cancer and bone metastases. BJU Int 2009;103:434–40.
37. Jallal H, Valentino ML, Chen G, Boschelli F, Ali S, Rabbani SA. A Src/Abl kinase inhibitor, SKI-606, blocks breast cancer invasion, growth, and metastasis *in vitro* and *in vivo*. Cancer Res 2007;67: 1580–8.
38. Nam S, Kim D, Cheng JQ, et al. Action of the Src family kinase inhibitor, dasatinib (BMS-354825), on human prostate cancer cells. Cancer Res 2005;65:9185–9.
39. Park SI, Gallick GE. c-Src activation in the tumor-associated endothelial cells contributes to the lymph node metastases of prostate cancer cells. Proc Am Assoc Cancer Res 2007;48:3002.
40. de Vries TJ, Mullender MG, van Duin MA, et al. The Src inhibitor AZD0530 reversibly inhibits the formation and activity of human osteoclasts. Mol Cancer Res 2009;7:476–88.

41. Zhang XH, Wang Q, Gerald W, et al. Latent bone metastasis in breast cancer tied to Src-dependent survival signals. Cancer Cell 2009;16: 67–78.
42. Hannon RA, Clack G, Rimmer M, et al. Effects of the Src kinase inhibitor saracatinib (AZD0530) on bone turnover in healthy men: a randomized, double-blind, placebo-controlled, multiple ascending dose phase I trial. J Bone Miner Res 2010;25:463–71.
43. Koreckij T, Nguyen H, Brown LG, Yu EY, Vessella RL, Corey E. Dasatinib inhibits the growth of prostate cancer in bone and provides additional protection from osteolysis. Br J Cancer 2009;101: 263–8.
44. Frame MC. Src in cancer: deregulation and consequences for cell behaviour. Biochim Biophys Acta 2002;1602:114–30.
45. Myoui A, Nishimura R, Williams PJ, et al. C-SRC tyrosine kinase activity is associated with tumor colonization in bone and lung in an animal model of human breast cancer metastasis. Cancer Res 2003;63:5028–33.
46. Wu Z, Chang P-C, Yang JC, et al. Autophagy blockade sensitizes prostate cancer cells towards Src family kinase inhibitors. Genes Cancer 2010;1:40–9.
47. Suh J, Rabson AB. NF-κB activation in human prostate cancer: important mediator or epiphenomenon? J Cell Biochem 2004;91: 100–17.